Bandgap Engineering by Cationic Disorder:

Case Study on $AgBiS_2$

Francesc Viñes,[a] Gerasimos Konstantatos,[b,c] and Francesc Illas[*,a]

[a] *Departament de Ciència de Materials i Química Física & Institut de Química Teòrica i Computacional (IQTCUB), Universitat de Barcelona, C/Martí i Franquès 1, 08028 Barcelona, Spain.*

[b] *ICFO-Institut de Ciències Fotòniques. The Barcelona Institute of Science and Technology, 08860 Castelldefels (Barcelona), Spain.*

[c] *ICREA-Institució Catalana de Recerca i Estudis Avançats. Passeig Lluís Companys 23, 08010 Barcelona, Spain.*

* francesc.illas@ub.edu

Abstract

The influence of cationic disorder on the electronic structure of ternary compounds, here exemplified on $AgBiS_2$ material, is studied by means of accurate first principles periodic density functional theory based calculations. For $AgBiS_2$ cationic disorder in going from semiconducting matildite to a metallic arrangement crystal structure is found to induce a significant decrease on the band gap, as a result from cation-disorder conduction band tail states penetrating into the matildite bandgap. Properly aligned conduction band minimum and valence band maximum shows that cationic disorders leads to a noticeable drop of the former and slight increase of the latter. The present results indicate that temperature effects triggering cationic disorder will have a beneficial effect on the photoactivity of $AgBiS_2$ samples provided that the metallic limit is not reached.

The scientific interest on mixed Silver-Bismuth sulphur ($AgBiS_2$), minerally named matildite, has recently been renewed given its outstanding performance in high-performance environmentally friendly solar cells,[1] yet was previously posed as sensitizer or counter-electrode in sensitized solar cells.[2,3] Other authors highlight its usage for thermoelectric power generation given its ultralow thermal conductivity.[4,5] Indeed, $AgBiS_2$ is just a textbook example of I-V-VI_2 family of compounds —I = Cu, Ag, or an alkali metal; V = Sb or Bi, and VI = S, Se, or Te—. The different polymorphs of such materials can be described using a cubic $Fm\bar{3}m$ type of crystallographic structure supercell, *i.e.*, a rocksalt arrangement of VI anions, where I and V cations are embedded in a specific arrangement, where specific primitive unit cells, such as the most stable $P\bar{3}m1$ of $AgBiS_2$ can be contained.

Many physicochemical properties of interest for practical applications actually rely on the specific cationic ordering inside the bulk material. Among this family of materials, $AgBiSe_2$ and $AgSbTe_2$ have been highlighted as excellent low-temperature thermoelectrics.[4,6,7] Such low-temperature thermoelectric materials are interesting as well as phase-change memory devices, and competition between different ground state cationic orderings on $AgBiTe_2$ has been pointed out as an efficient phonon scatter.[8] In the particular case of $AgBiSe_2$ it has been observed that the thermoelectric power seems to be affected by temperature, especially when other phases of this material, involving some degree of cation disorder, are sampled.[6] Moreover, $AgBiS_2$ high thermoelectric power is found to be heavily decimated at around 610 K, a temperature in which its well-defined matildite crystal structure transforms into a cation disordered one.[2,9]

Such property change with respect the cationic ordering may well be interpreted based on the band broadening of disordered systems. Notice that bandgap reduction is experimentally observed *i.e.* when thermalizing,[10] and is conceptualized based on Urbach tails, where valence band features an exponential decaying tail appearing when band dispersion is suppressed as a result of the material disordering. Urbach tails are found when disorders or impurities as significant,[11] and should be discerned to point defects, such as low-concentration vacancies, which display discrete states within the otherwise unchanged materials bandgap.[12] Such tails are interpreted in terms of thermal fluctuations arising from temperature-dependent coupling of excitons and phonons,[13] although other authors affirm that the origin stems out from a dependence of the

bandgap with respect an appearing tail of the density of states (DOS) when having disordered systems.[14]

Related to the above point, here we show that the photochemical response of $AgBiS_2$ is highly dependent on the specific cation arrangement, *i.e.* the cationic disorder, and suggest that this disorder can be thermally controlled at will to fine-tune the light absorbance spectrum and band edge positions. Previously, it has been shown that matildite $AgBiS_2$ is a semiconductor, whereas another specific well-defined cationic arrangement of this material, containing parallel squared Ag-S and Bi-S planes, is metallic.[15] Here we hypothesize that other cationic ordering may be considered as middle states in between these two extreme cases. To prove that, accurate *ab initio* density functional theory (DFT) simulations have been carried out for the semiconductor (matildite) and metallic limit cationic arrangements, as well as for a total of 26 different cationic disorders, randomly generated by successive Ag-Bi site permutations within the crystal unit cell. Notice that such a large phase sampling ensures a proper description of the structural diversity when cations are free to exchange their positions, as observed at the phase transition temperature of 610 K,[9] and well surpasses previous analysis of cationic arrangement on I-V-VI_2 compounds, where only a few specific positions, still with a high degree of ordering, were contemplated,[8-16] thus biasing the results to a very narrow region of the configurational space.

The cationic disorders have been applied on the cubic, rocksalt like, unit supercells of matildite and the metallic ordering, see Fig. 1, containing 32 S, and 16 Ag and Bi atoms. For each structure, unit cell dimensions and atomic positions have been optimized so as to feature an internal pressure under 1 bar and forces acting on atoms below 0.01 eV $Å^{-1}$. Briefly, DFT based calculations have been carried out using the Perdew-Burke-Ernzerhof (PBE) exchange correlation potential,[17] with the valence electron density expanded in a plane wave basis set with a kinetic energy cutoff of 415 eV, and a reciprocal space Monkhorst-Pack **k**-point sampling using a 5×5×5 grid; further computational details are found elsewhere.[15] The bandgaps, E_g, are obtained from the difference in energy of the valence band maximum (VBM) and conduction band minimum (CBM), extracted from the systems DOS with an energy resolution of 0.001 eV. Notice that from a rigorous point of view E_g should be obtained from appropriate quasi-particle calculations as in the *GW* approach;[18] below we tackle this issue.

It is worth pointing out that DFT based calculations with the PBE functional severely underestimate the E_g values due to the known self-interaction error. The use of the hybrid functionals, adding a fraction of non-local, exact, Fock exchange, such as Heyd-Scuseria-Ernzerhof (HSE06),[19] overcomes this limitation, generally resulting in values closer to experiment.[20] Using the HSE06 functional matildite is predicted to exhibit a bandgap of 1.54 eV, close to recent experimental estimates in the range of 1.1-1.32 eV,[1,3,21-23] whereas the metallic arrangement is preserved even when carrying out HSE06 calculations on top. The overall good performance of HSE06 in predicting band gap values[20] provides the required confidence on the observed trend, regardless of the PBE underestimation. In the following, the PBE E_g estimates are scaled to the results predicted by the more accurate HSE06 hybrid functional using previously obtained HSE06 results on the matildite and metallic solutions for so,[15] yet energetics is treated at the already realistic PBE level.

As shown in Fig. 1 any cationic exchange from matildite tessellated structure implies a structure higher in energy, as evidenced by the difference in total energy per $AgBiS_2$ unit, ΔE, between the (semi)disordered structure and that of matildite. On the other hand, any cationic exchange from the metallic ordering is energetically beneficial. Therefore, it seems as metallic $AgBiS_2$ represents indeed a limit of stability. All other partially disordered structures exhibit ΔE values in between these two limit polymorphs of $AgBiS_2$. Notice in Fig. 1 insets how the internal ordering is perfectly defined in the limit cases, although interatomic distances become somewhat disrupted for intermediate situations. In any case, the overall $Fm\bar{3}m$ crystallographic arrangement is maintained, that is, no other internal arrangements are observed, with the exception of matildite $P\bar{3}m1$ one.

Another important feature observed in Fig. 1 is that it evidences a clear trend of the calculated E_g when going from the semiconductor to metallic solutions. Thus, simple Ag-Bi swap exchanges decimate not only stability with respect matildite, but also the energy bandgap with none of the explored situations enlarging this property. Thus, evidently, when one anneals matildite $AgBiS_2$, cationic disorder is triggered, making other metastable minima reachable displaying different cationic ordering, and effectively reducing the materials bandgap. This is particularly achievable given the close energetic proximity of the semi(disordered) phases. The reason for such E_g decay

seems to be the appearance of a DOS tail in the conduction band in accordance to the above-commented Urbach tails.[14] Fig. 2 shows the PBE DOS of matildite and metallic limit situations, scaled to their respective Fermi levels, as well as selected intermediate (semi)disordered situations. Clearly, the inclusion of disorder broadens the conduction band, placing a DOS tail into the matildite bandgap. The higher the disorder, the deeper sinks the tail into the bandgap, up to reaching the metallic limit situation. Notice that while the conduction band is broadened is flattened, the valence band remains tail-free and essentially unperturbed, with a somewhat narrowing, at most, in accordance with the above-commented trend on other semiconductors.[26]

This is further illustrated in Fig. 3 with the atom-decomposed bandstructure **Γ**-centred plots of valence and conduction bands near the Fermi level. Clearly, the inclusion of a small degree of cationic disorder already disrupts the very nature of the semiconductor bandgap, transforming it from an indirect gap[15] to a direct gap semiconductor located at **Γ** point. Moreover, the addition of more cationic disorder reduces the bandgap at Γ, where the above-commented lowering of CBM becomes evident, as well as the essentially unperturbed VBM band edge. Notice as well the bands dispersion flattening when cationic disorder is introduced. Last but not least, the Bi *sp* character of the conduction band becomes S *sp* alongside the bandgap narrowing, to a final mixture and conversion at the metallic solution.

Given the observed trend, the cationic (dis)ordering can be effectively used to reduce the materials bandgap, serving as a counterbalance to the observed bandgap increase by matildite $AgBiS_2$ nanostructuring as observed on $AgBiS_2$ nanoparticles, where, due to quantum confinement effects, E_g values of 2.67 eV on quantum dots of 8.5 ± 1.2 nm size are observed,[24] or a reported value of 2.78 eV is obtained for a sample of nanoparticles of average 7.6 nm size.[25] However, the observed decrease of the E_g with respect disorder is not linear, and, for a given reachable energy window, many bulk orderings are possible, with a diversity of associated bandgaps. Therefore, a statistically averaged bandgap reduction is to be expected, unless the disorder is externally induced or kinetically controlled.

This overall trend is not necessarily unique to $AgBiS_2$, but probably the case of other I-V-VI_2 compounds displaying a lowest in energy matildite semiconductor type of structure and a highest in energy metallic type. Previous DFT estimates using a similar

functional to PBE pointed this to be the case for $AgSbTe_2$ and $AgSbSe_2$,[16] but not $AgSbS_2$, where most stable polymorph is already metallic. Clearly composition, the existence of polymorphism, and the different cationic arrangements within the bulk solid are key features to fine-tune the electronic structure in general, and the bandgap in particular, on this class of materials.

As far as disorder is concerned, notice that, given that all cationic sites could well be indistinctly occupied by either Ag or Bi atoms, an aspect of interest would be whether the configurational entropy could play a key role in the stabilization of such disordered phases. The number of combinations of Ag and Bi cations within the employed unit supercell is $32!/(16!)^2$. Notice that such large amount of possibilities is unreachable, even when one could reduce the number by equivalent situations. Indeed, a gross approximation to reduce equivalent configurations would be to divide the number of combinations by the $Fm\bar{3}m$ total number of symmetry operations, thus assuming that periodic crystal symmetry is maintained although disorder effectively reduces the total number of symmetry operations, but even in that case the sampling would be unreachable. Another possibility would be to sample a larger amount of possibilities as a representative set of reality and fit it to a model distribution, but even here the required distribution is far beyond what can be achieved nowadays. Thus, we decide to explore the maximum configurational entropy stabilization limit case by considering no reduction by crystal symmetry and considering all situations equally reachable. Then, according to Boltzmann entropy formula $S=k_B \cdot \ln W$, the estimated entropy reduction to the Gibbs free energy at 610 K would be of 0.066 eV per formula unit. Notice that this idealized maximum stabilization is to be heavily hindered for situations with low degeneracy, such as matildite and the ordered metallic solution, but can be significant in the intermediate situations with higher disorder. However, given the higher energy of disordered cases and the symmetry point operations applicable, in the real case such entropy stabilization would be significantly reduced. Thus, yet accounting for only a few meV per formula unit, configurational entropy contribute in defining the stabilization and sampling of (semi)disordered situations at finite temperatures.

A remaining question mark is how the above-commented E_g reduction by cationic disorder is accompanied by a band edge level alteration, as seen in Fig. 3. To further investigate this in more detail, the VBM and CBM of matildite, the metallic limit, and all semi(disordered situations) obtained from the corresponding DOS have

been aligned taking as reference the mean energy value for the deepest Bi 1*s* core level, a strategy used in a previous work involving several ZnO polymorphs.[26] In addition, the VBM of matildite has been taken as a common zero energy reference, and the E_g estimates scaled to the results predicted by the more accurate HSE06 hybrid functional to avoid unrealistic band edge crossings.

Fig. 4 reports the corresponding aligned results and show that VBM and CBM are placed well apart in the highly ordered matildite semiconductor crystal, whereas for the metallic structure both band edges coincide at an energy in between the band limits of matildite. This latter crystal domains, when present, could serve as electron/hole recombination centres of light triggered excitons in $AgBiS_2$ samples, yet, luckily, are the highest energy limit. Even more interesting are the more reachable-in-energy intermediate (semi)disordered situations where a clear CBM drop is observed, together with a slight increase in energy of VBM. This goes along with previous studies in which CBM position was more affected than VBM when structural changes are applied, as CBM state features a more dispersion than VBM, and, consequently, structural disruptions localizing states are more prone to flatten CBM than VBM.[15,26] Notice that CBM is found to be mainly composed by overlapping Bi *sp* states, which, given their diffusive nature, favour such couplings and are the origin of a higher dispersion of the band compared to VBM, mainly composed or more localized S *sp* states.

In any case, a clear trend towards schapbachite is clearly observed although the implications of VBM and CBM position in these particular cationic arrangements are different: Given that at moderate temperatures these intermediate, partially disordered, situations would be present in $AgBiS_2$ samples, the different excitation/deexcitation energy for electrons and remaining holes suggests a distinct rate of dispersion over the material which would be translated into a more inefficient exciton recombination, and, therefore, a better photochemical activity, thus supporting, although in an indirect way, the efficient $AgBiS_2$ photoactivity found in slightly disordered $AgBiS_2$ samples, where a disordered cationic arrangement is intuited from X-ray diffraction patterns.[1]

In summary, we have shown here that the photochemical response of bulk $AgBiS_2$ is highly dependent on the specific cation arrangement, *i.e.* the cationic disorder. Arrangements different from the highly ordered matildite are accessible in energy, fostered by a configurational entropy energy stabilization, as observed in the

phase change temperature of 610 K, with the metallic crystal structure being the highest energy limit. Notice in passing by that the energetic feasibility of such disorders may be affected by surface effects on nanocrystallite materials, where here only bulk aspects are considered. However, the bulk (semi)disordered arrangements feature a reduced bandgap E_g, and a substantial reduction of the CBM edge, with a slight increase of the CBM. This different (de)stabilization of the band edge limits is to be a key determinant factor in allowing for the survival of light-triggered excitons, and therefore, help to explain the efficient $AgBiS_2$ photoactivity. Yet, the existence of highest-in-energy metallic domains could serve as recombination centres. Therefore, only slight disorders from matildite are to be considered useful for optoelectronic devices.

Acknowledgements: This work has been supported by Spanish Ministry of Economy and Competitiveness (MINECO) and *Fondo Europeo de Desarrollo Regional* (FEDER) CTQ2015-64618-R and MAT2014-56210-R grants and partly by *Generalitat de Catalunya* grants 2014SGR97, 2014SGR1548, and XRQTC, the *Fundación Privada Cellex*, and the European Community Seventh Framework Programme (FP7-ENERGY.2012.10.2.1) under agreement N^o 308997. The research in this work is in the framework of the NOMAD Center of Excellence project, which received funding from the European Union's Horizon 2020 research and innovation programme under grant agreement N^o 676580. F.V. thanks MINECO for a postdoctoral *Ramón y Cajal* (RyC) research contract (RYC-2012-10129). F.I. acknowledges additional support from the 2015 ICREA Academia Award for Excellence in University Research. G.K. acknowledges financial support from the Spanish Ministry of Economy and Competitiveness, through the *Severo Ochoa* Programme for Centres of Excellence in R&D (SEV-2015-0522).

Fig. 1. Bandgap, E_g, variation (as HSE06 corrected on PBE estimates) as a function of the energy difference, ΔE, per $AgBiS_2$ unit (from PBE estimates), of cation disordered structures with respect matildite arrangement. Insets depict initial matildite, final metallic solution, and some intermediate structures. Grey, pink, and yellow spheres denote Ag, Bi, and S atoms, respectively. Yellow background guides the eye on the configurationally explored region.

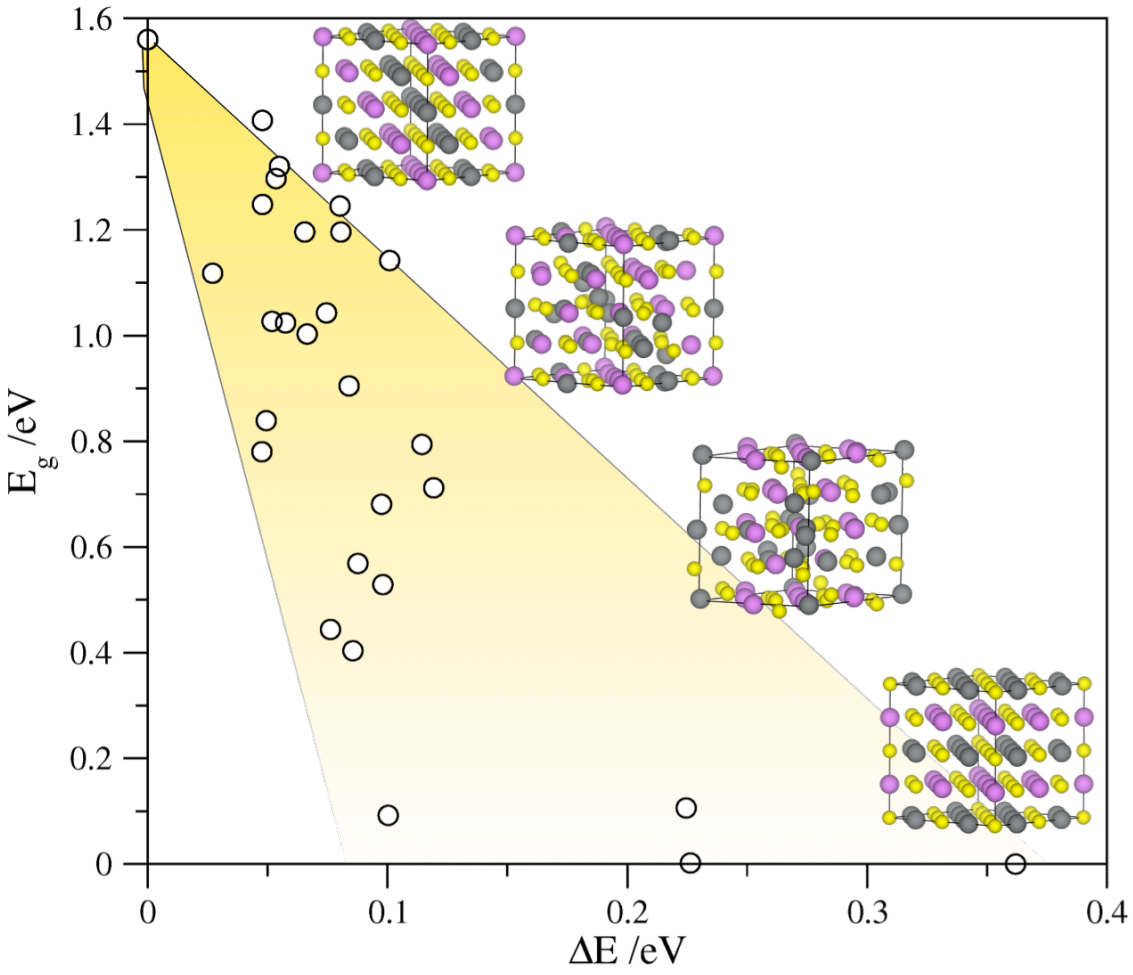

Fig. 2. Total DOS of $AgBiS_2$ semiconductor matildite (black), of the metallic limit (orange) and selected cation semi-disordered situations encompassing intermediate situations as found in Fig. 1.

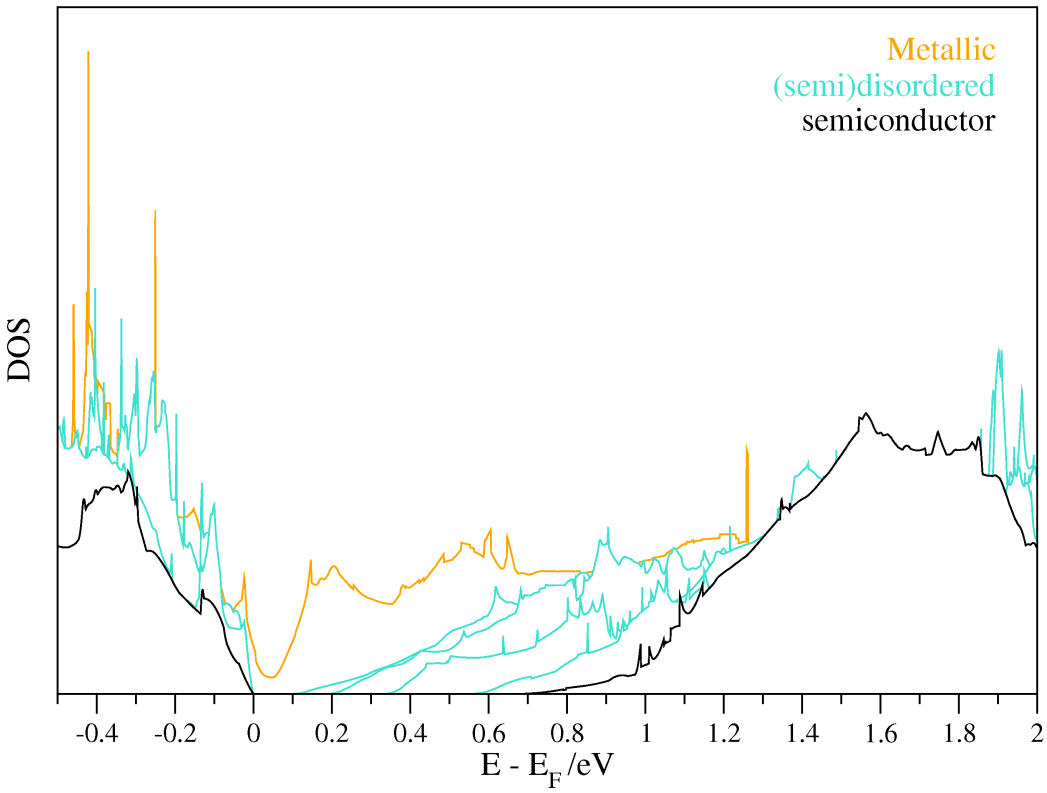

Fig. 3. Bandstructures nearby **Γ** point —± 0.1 $Å^{-1}$— in the energy range of ± 1 eV from E_F for the situations shown in Fig. 2. Color code follows atomic contributions as in Fig. 1, where sphere sizes relate to the particular atomic quantitative contribution.

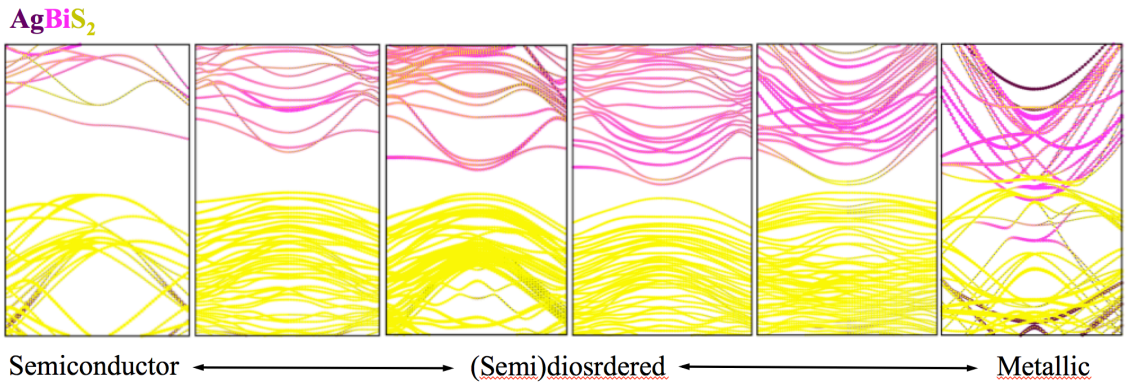

Fig. 4. Conduction Band Minimum (CBM) and Valence Band Maximum (VBM) energy levels, HSE06 corrected, and aligned with respect to average Bi (1*s*) core level binding energy, for matildite (left), schapbachite (right), and (semi)disordered situations (in between), as a function of the energy difference per $AgBiS_2$ unit with respect matildite phase. Notice that matildite VBM is taken as zero energy reference. All values are given in eV. Colored background is an eye guide to the observed trend.

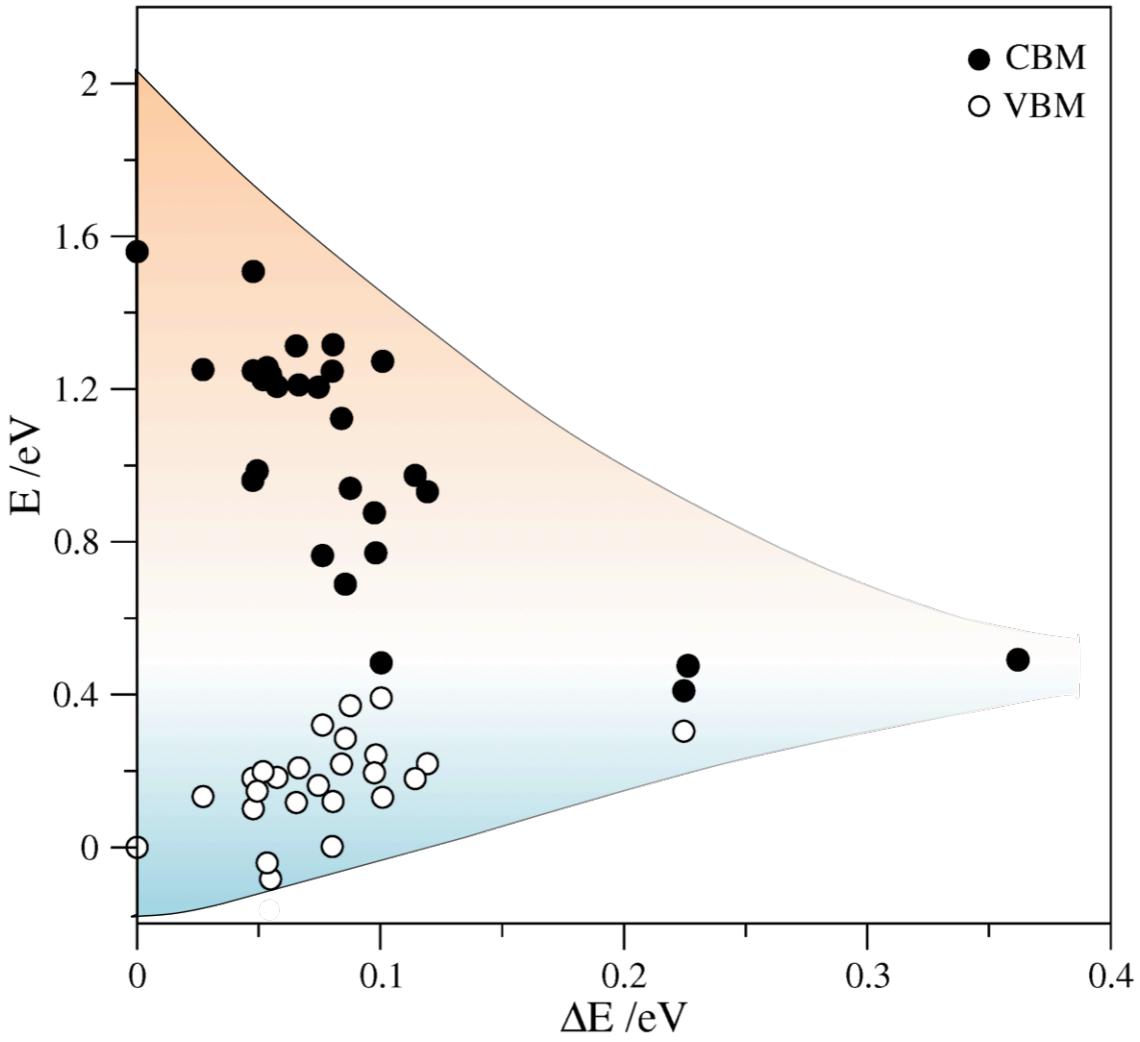

References:

1 M. Bernechea, N. C. Miller, G. Xercavins, D. So, A. Stavrinadis and G. Konstantatos, *Nat. Photon.*, 2016, **10**, 521-525.

2 S.N. Guin and K. Biswas, *Chem. Mater.*, 2013, **25**, 3225-3231.

3 B. Pejova, D. Nesheva, Z. Aneva and A. Petrova, *J. Phys. Chem. C*, 2011, **115**, 37-46.

4 S.N. Guin, A. Chatterjee, D.S. Negi, R. Datta and K. Biswas, *Energy Environ. Sci.*, 2013, **6**, 2603-2608.

5 C. Xiao, X. Qin, J. Zhang, R. An, J. Xu, K. Li, B. Cao, J. Yang, B. Ye and Y. Xie, *J. Am. Chem. Soc.*, 2012, **134**, 18460-18466.

6 S.N. Guin, V. Srihari and K. Biswas, *J. Mater. Chem. A*, 2015, **3**, 648-655.

7 D.T. Morelli, V. Jovovic and J.P. Heremans, *Phys. Rev. Lett.*, 2008, **101**, 035901.

8 J. Ma, O. Delaire, A.F. May, C.E. Carlton, M.A. McGuire, L.H. VanBebber, D.L. Abernathy, G. Ehlers, T. Hong, A. Huq, W. Tian, V.M. Keppens, Y. Shao-Horn and B.C. Sales, *Nat. Nanotechnol.*, 2013, **8**, 445-451.

9 S.N. Guin, S. Banerjee, D. Sanyal, S.K. Pati and K. Biswas, *Inorg. Chem.*, 2016, **55**, 6323-6331.

10 M.V. Kurik, *Phys. Stat. Sol.*, 1971, **8**, 9-45.

11 A.R. Zanatta and I. Chambouleyron, *Phys. Rev. B*, 1996, **53**, 3833-3836.

12 F. Viñes and F. Illas, *J. Comput. Chem.*, 2017, **38**, 523-529.

13 T. Skettrup, *Phys. Rev. B*, 1978, **18**, 2622-2631.

14 S. John, C. Soukolis, M.H. Cohen and E.N. Economou, *Phys. Rev. Lett.*, 1986, **57**, 1777-1780.

15 F. Viñes, M. Bernechea, G. Konstantatos and F. Illas, *Phys. Rev. B*, **94**, 234203 (2016).

16 K. Hoang, S.D. Mahanti, J.R. Salvador and M.G. Kanatzidis, *Phys. Rev. Lett.*, 2007, **99**, 156403.

17 J.P. Perdew, K. Burke and M. Ernzerhof, *Phys. Rev. Lett.*, 1996, **77**, 3865-3868.

18 J. P. Perdew, W. Yang, K. Burke, Z. Yang, E. K. U. Gross, M. Scheffler, G. E. Scuseria, T. M. Henderson, I. Y. Zhang, A. Ruzsinszky, H. Peng, J. Sun, E. Trushin and A. Görling, *Proc. Natl. Acad. Sci.*, 2017, **114**, 2801-2806.

19 J. Heyd, G.E. Scuseria and M. Ernzerhof, *J. Chem. Phys.*, 2003, **118**, 8207.

20 A. J. Garza and G. E. Scuseria. *J. Phys. Chem. Lett.*, 2016, **7**, 4165-4170.

21 P.-C. Huang, W.-C. Yang, and M.-W. Lee, *J. Phys. Chem. C* 2013, **117**, 18308-18314.

22 D. Nesheva, Z. Aneva, B. Pejova, I. Grozdanov and A. Petrova, *J. Optoelectron. Adv. M.*, 2009, **11**, 1347-1350.

23 B. Pejova, I. Grozdanov, D. Nesheva and A. Petrova, *Chem. Mater.*, 2008, **20**, 2551-2565.

24 C. Chen, X. Qiu, S. Ji, C. Jia and C. Ye, *CrystEngComm*, 2013, **15**, 7644-7648.

25 N. Liang, W. Chen, F. Dai, X. Wu, W. Zhang, Z. Li, J. Shen, S. Huang, Q. He, J. Zai, N. Fang and X. Qian, *CrystEngComm* 2015, **17**, 1902-1905.

26 I. Demiroglu, S. Tosoni, F. Illas and S.T. Bromley, *Nanoscale*, 2014, **6**, 1181-1187.